JOURNAL OF MATERIALS SCIENCE 27 (1992) 5735–5738

Hydrogen trapping and repelling in an Al–6 wt% Zn–2 wt% Mg alloy

YOSHIAKI IIJIMA, SHIN-ICHI YOSHIDA*, HIDEYUKI SAITOH‡, HIROSHI TANAKA§, KEN-ICHI HIRANO
Department of Materials Science, Faculty of Engineering, Tohoku University, Aoba, Sendai 980, Japan

Hydrogen trapping in an Al–6 wt % Zn–2 wt % Mg alloy aged up to typical stages in the age-hardening curve has been studied by measuring the tritium release rate after charging. The distribution of hydrogen in the aged alloy has been studied by tritium electron microautoradiography. It has been found that the Guinier–Preston zones in the alloy do not act as trapping sites but as a repeller for hydrogen, and that η′ precipitate does not trap hydrogen, but the interface between the matrix and η precipitate acts as a trapping site for hydrogen. Dislocation has been found to be capable of trapping hydrogen, while trapped hydrogen by the grain boundary has not been observed.

1. Introduction

Al–Zn–Mg is known as one of the strongest age-hardenable aluminium alloys and it is widely used as a high-strength structural material. However, the sensitivity of this alloy to stress-corrosion cracking is relatively high, and it has been connected with the behaviour of hydrogen [1, 2]. The precipitation process of a supersaturated Al–Zn–Mg alloy is known to be [3–6]: supersaturated solid solution → sphere-like Guinier–Preston (GP) zone → plate-like metastable precipitate (η′ phase, $MgZn_2$) → plate-like or rod-like equilibrium precipitate (η phase, $MgZn_2$), and wide variations of metallographic microstructure, as well as lattice defects such as dislocations and grain boundaries, can be formed by ageing a supersaturated alloy. Thus, it is very interesting to examine the interactions between hydrogen and each of the microstructures.

Tritium electron microautoradiography is a unique and useful technique which can provide visual information on the interrelationship between hydrogen distribution and microstructure. Tritium emits only low-energy β-rays with a continuous energy spectrum (maximum energy 18.6 keV) with a half-life of 12.3 year. The maximum range of the β-rays of tritium through photographic emulsion (silver bromide) and aluminium is 2.5 and 2.7 μm, respectively, and 99% of the energy is absorbed on passing through these materials by about 0.4 μm [7]. Thus, the spatial resolution for the tritium distribution in the specimen of the autoradiograph is very high. A sensitive film is adhered to the specimen and exposed to the β-rays from tritium charged in the specimen. The film is then developed, and the distribution of silver grains in the film is examined by an electron microscope. So far, this technique has been applied by us to pure aluminium and aluminium alloys such as Al–Mg–Si [8, 9] and Al–Cu [9] to identify the trapping and repelling sites of hydrogen in them.

In the present work, first the age-hardening curve of the alloy at 160 °C has been determined. Secondly, the intensity of trapping hydrogen in the specimens aged up to typical stages in the age-hardening curve has been studied by measuring the tritium release rate after charging. Finally, the interrelationship between hydrogen distribution and microstructures with lattice defects and precipitates has been investigated by tritium electron microautoradiography.

2. Experimental procedure

A sheet of Al–6 wt % Zn–2 wt % Mg alloy was supplied by Sumitomo Light Metal Industries Ltd. Contents of zinc and magnesium in it were 5.98 and 2.03 wt %, respectively. The main impurities were Fe: 0.01 and Si: < 0.01 wt %. Foil specimens 5 mm × 5 mm × 0.2 mm in size were sealed in a glass tube with argon gas and were solution heat-treated at 500 °C for 7.2 ks and then quenched into ice water. Subsequently, the specimens were aged at 160 °C in an oil bath. After ageing, the specimens were kept in a refrigerator at − 10 °C. Hardness of the specimen was measured by a Vickers microhardness tester at room temperature with 200–1000 g loading. All the readings were averaged on eight impressions.

Tritium and hydrogen were charged into the specimens at room temperature by the cathodic charging

* *Present address*: Seiko Instruments Inc., Kameido, Tokyo 136, Japan.
‡ *Present address*: Department of Materials Science and Engineering, Faculty of Engineering, Kyushu University, Fukuoka 812, Japan.
§ *Present address*: Nippondenso Co. Ltd, Kariya 448, Japan.

0022–2461

method. The electrolyte was 0.5 N H_2SO_4 aqueous solution containing tritium of 3.7×10^{13} Bq m^{-3}, the current density and charging time being 100 A m^{-2} and 3.6 ks, respectively. After charging each specimen was rinsed with water and ethyl alchohol and put into a scintillator solution (Scintisol 500) within 5 min after the charging and held in it for 24 h. The radioactivity of tritium released from the specimen into the scintillator solution was measured for 2 h by a liquid scintillation counter.

For the tritium electron microautoradiography, tritium and hydrogen were charged into the specimens by the same method as above. After charging, each specimen was kept at -10 °C for 3 days to release excess hydrogen and to attain an equilibrium distribution of hydrogen. Discs 3 mm in diameter were cut from the specimen and polished into thin foils by the twin jet method using a solution of 7 parts C_2H_5OH and 1 part $HClO_4$ as an electrolyte at 0 °C. The electrolytic voltage was 30 V. A sensitive film made of a monolayer of fine silver bromide grains 0.06 μm in diameter was prepared on collodion thin films by the wire-loop method from a nuclear photographic emulsion (Konica NR-H2). One or two drops of isoamyl acetate were put on the specimen to adhere the sensitive film to the specimen. The set of the sensitive film and the specimen was kept in a dark box maintained at -10 °C for 6 days to expose the sensitive film to the β-rays emitted from tritium in the specimen.

After exposure, the sensitive film on the specimen was developed to turn the silver bromide grains exposed by the β-rays into metallic silver grains. Thus, information on the distribution of hydrogen in the specimen could be obtained by observing the distribution of silver grains in the autoradiograph. To make simultaneous observation of both the hydrogen distribution and the microstructure of the specimen, the specimen and the autoradiograph adhered to it were observed at the same time by transmission electron microscopy (TEM, Jeol-200B) at an accelerating voltage of 200 kV.

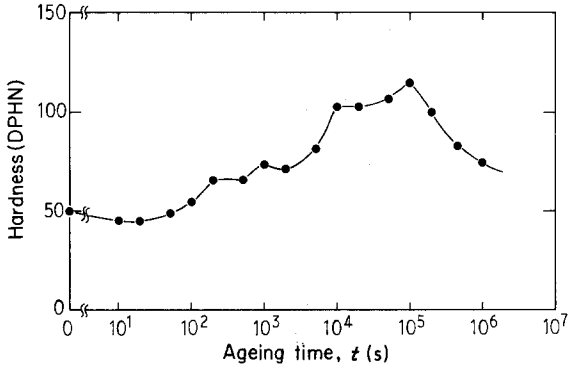

Figure 1 Age-hardening curve of Al–6 wt % Zn–2 wt % Mg alloy aged at 160 °C after quenching from 500 °C.

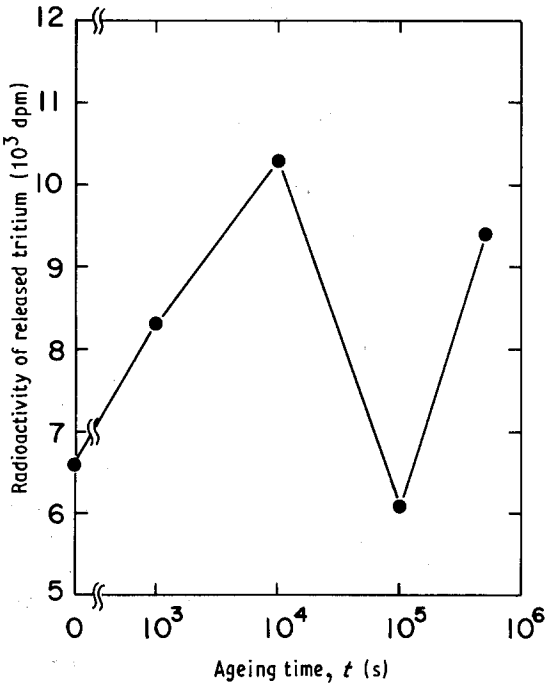

Figure 2 Radioactivity of tritium released from Al–6 wt % Zn–2 wt % Mg alloy measured by a liquid scintillation counter.

3. Results and discussion

Fig. 1 shows the age-hardening curve of the Al–6 wt % Zn–2 wt % Mg alloy aged at 160 °C. The hardness value of the as-quenched specimen was 50. After an incubation time of about 100 s, the hardness starts to increase gradually and has a plateau of about 65 during ageing for 2 ks. Beyond the plateau region, the hardness increases again rapidly to a value of about 100 which forms a second plateau including a maximum at the ageing time 100 ks, and finally decreases gradually with ageing time. According to studies on the precipitation process of the alloy [3–5], the first hardness plateau during the ageing for 2 ks is due to the formation of GP zones and η′ precipitates. The second plateau including the maximum of hardness is mainly due to the formation of η′ and η precipitates. The over-ageing after the maximum is due to the growth of η precipitates.

Tritium release experiments are shown for the as-quenched specimen and also for aged specimens at typical states in Fig. 2. Tritium charging for all the specimens was carried out under the same conditions. As shown in Fig 2, the radioactivities of tritium released from the as-quenched specimen and from the specimen aged for 100 ks are much lower than those from the specimens aged for 10 and 500 ks. High radioactivity of released tritium from a specimen means that most of the previously charged tritium is released and only a part of the tritium remains in the specimen, and vice versa. Fig. 2 shows that the intensities of trapping hydrogen in both the as-quenched specimen and the specimen aged for 100 ks are strong, while on the other hand those in the specimens aged for both 10 and 500 ks are weak. Thus, in the as-quenched specimen, it appears that vacancy-rich clusters [6] trap hydrogen. The trapping power in the aged specimens decreases with the formation of GP zones and η′ precipitates. However, as shown in Fig. 2, with an increase of η precipitates the trapping power increases, but it again decreases with the growth of η precipitates in the over-aged state.

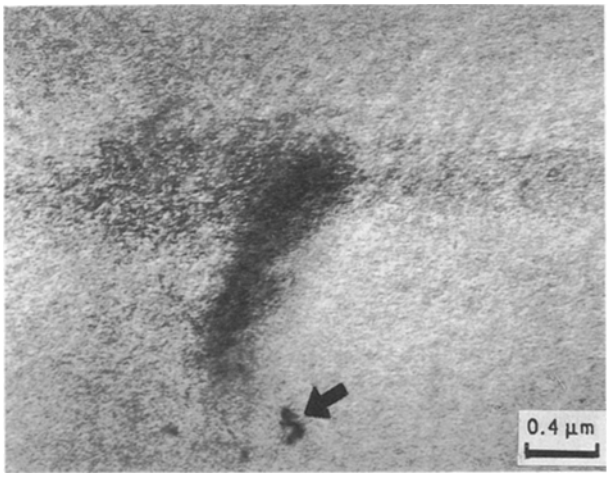

Figure 3 Tritium electron microautoradiograph of Al–6 wt % Zn–2 wt % Mg alloy aged at 160 °C for 1 ks after quenching. A silver grain is observed at the end of a dislocation, as shown by the arrow.

Figure 4 Tritium electron microautoradiograph of Al–6 wt % Zn–2 wt % Mg alloy aged at 160 °C for 10 ks after quenching. Silver grains are observed at the interface between the matrix and the unresolved rod-like η precipitates, as shown by arrows.

Fig. 3 shows a tritium electron microautoradiograph of Al–6 wt % Zn–2 wt % Mg alloy aged at 160 °C for 1 ks after quenching. Sphere-like GP zones with a high density are observed. However, silver grains are only rarely seen and a definite relationship between the sites of the silver grains and those of the GP zones is hardly found. This suggests that the GP zones in this alloy have no trapping power for hydrogen. The silver grain indicated by the arrow appears to be located at the termination of a dislocation on the surface of the specimen. According to Gerold and coworkers [3, 10], the GP zones in Al–6 wt % Zn–2 wt % Mg alloy have coherency with the matrix lattice and cause a compressive elastic stress field in the matrix around them. This compressive stress field acts as a repeller for hydrogen, as in the case of the GP zones in Al–Mg–Si alloy [8, 9]. In contrast to the GP zones in Al–Zn–Mg and Al–Mg–Si alloys, the GP zones in Al–Cu alloy cause a tensile elastic stress field in the matrix around them. This tensile stress field also acts as a trapping site for hydrogen [9].

Fig. 4 shows a tritium electron microautoradiograph of Al–6 wt % Zn–2 wt % Mg alloy aged at 160 °C for 10 ks after quenching. A so-called precipitate-free zone is observed on both the sides of the grain boundary which lies from the upper left side to the lower right side. Apart from the precipitate-free zone, plate-like η′ precipitates with a high density are observed. Silver grains are observed at the interface between the matrix and the large unresolved rod-like η precipitates. However, no silver grain is observed in any other location, suggesting that η′ precipitate as well as the GP zone does not trap hydrogen. This is consistent with the finding that η′ precipitate has coherent interface boundaries with the aluminium matrix but has no stress field around itself in the matrix [11].

Fig. 5 shows a tritium electron microautoradiograph of Al–6 wt % Zn–2 wt % Mg alloy aged at 160 °C for 100 ks after quenching to attain the state of maxium hardness (Fig. 1) by the precipitation of plate-like η′ and plate-like or rod-like η. Silver grains are

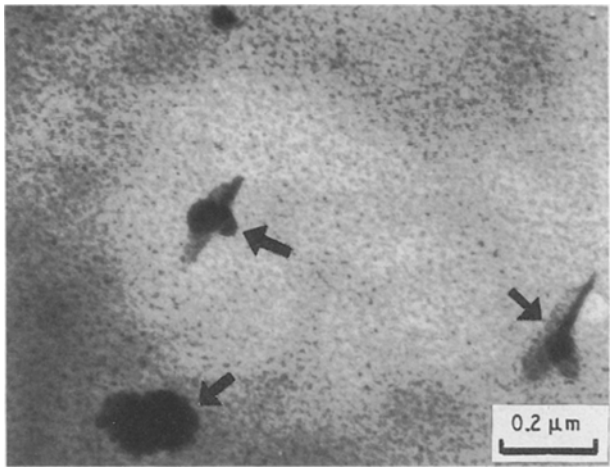

Figure 5 Tritium electron microautoradiograph of Al–6 wt % Zn–2 wt % Mg alloy aged at 160 °C for 100 ks after quenching. Silver grains are observed at the interfaces between the matrix and η precipitates, as shown by arrows.

observed at the interface between the matrix and η precipitates but not at the interfaces between the matrix and η′ precipitates which exist with a high density. The equilibrium η precipitate has incoherent interphase boundaries with the aluminium matrix. It has been found that three types of orientation relation between the matrix and η precipitates are mainly observed out of the eleven possible types [12, 13]. In the present experiment, however, determination of the orientation relation between them has not been carried out.

Fig. 6 shows a tritium electron microautoradiograph of Al–6 wt % Zn–2 wt % Mg alloy aged at 160 °C for 500 ks after quenching to obtain over-aged state (Fig. 1). In Fig. 6, large η precipitates on the grain boundary are observed, and a few silver grains are observed at the interfaces between the matrix and η precipitates, as shown by arrows. However, no silver grain is observed on the high-angle grain boundary of the matrix itself if the η precipitate does not exist. This indicates that the trapping power of the high-angle

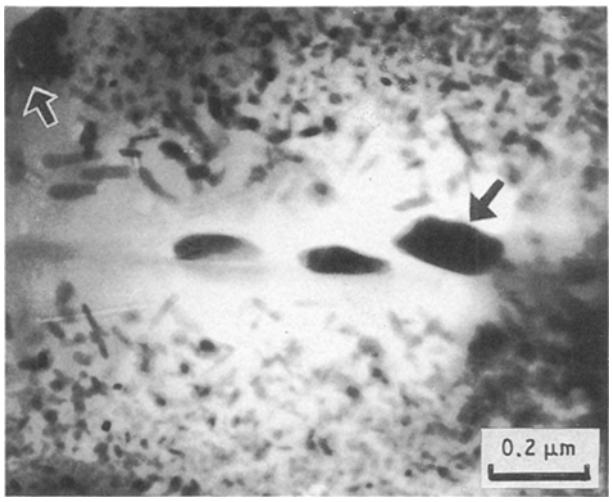

Figure 6 Tritium electron microautoradiograph of Al–6 wt % Zn–2 wt % Mg alloy aged at 160 °C for 500 ks after quenching, A few silver grains are observed at the interfaces between the matrix and η precipitates, as shown by arrows.

grain boundary is very weak or negligible. This is probably due to zero or very weak elastic interaction between the grain boundary and hydrogen.

4. Conclusions

The present experimental results are summarized as follows:

1. Dislocation in aluminium alloys acts as a trapping site for hydrogen and also acts as a short-circuiting diffusion path for hydrogen.
2. The GP zones in Al–6 wt % Zn–2 wt % Mg alloy do not act as a trapping site but as a repeller for hydrogen. η′ precipitate does not trap hydrogen.
3. The interface between the matrix and η precipitate acts as a trapping site for hydrogen.
4. The high-angle grain boundary in the matrix itself has zero or very weak trapping power for hydrogen.

Acknowledgements

The authors wish to thank Sumitomo Light Metals Industries Ltd for supply of Al–6 wt % Zn–2 wt % Mg alloy. This work was supported by a Grant-in-Aid for Fusion Research (62050015, 63050018, 01050028) from the Ministry of Education, Science and Culture. The authors would like to thank Professor M. Okamoto of Tokyo Institute of Technology and Professor M. Nishikawa of Kyushu University for their continuing interest and encouragement throughout the present work.

References

1. W. GRUHI and D. BRUNGS, *Metall* **23** (1969) 1020.
2. R. J. GEST and A. R. TROIANO, *Corrosion* **30** (1974) 274.
3. H. SCHMALZRIED and V. GEROLD, *Z. Metallkde* **49** (1958) 291.
4. A. KELLY and R. B. NICHOLSON, *Prog. Mater. Sci.* **10** (1963) 149.
5. K. ASANO and K. HIRANO, *Trans. Jpn Inst. Metals* **9** (1968) 24.
6. H. LÖFFLER, I. KOVÁCS and J. LENDVAI, *J. Mater. Sci.* **18** (1983) 2215.
7. J. P. LAURENT and G. LAPASSET, *J. Appl. Rad. Isotopes* **24** (1973) 213.
8. H. SAITOH, Y. IIJIMA and K. HIRANO, *J. Jpn Inst. Light Metals* **36** (1986) 286.
9. *Idem.*, in Proceedings of 4th International Conference on Hydrogen and Materials, Beijing, May 1988, edited by N. P. Chen and P. Y. Azou (ISCMCM, Saint Ouen, 1989) p. 647.
10. V. GEROLD and H. HABERKORN, *Z. Metallkde* **50** (1959) 568.
11. R. B. NICHOLSON, G. THOMAS and J. NUTTING, *J. Inst. Metals* **87** (1958–59) 429.
12. J. GJØNNES and C. J. SIMENSEN, *Acta Metall.* **18** (1971) 881.
13. H. P. DEGISCHER, W. LACON, A. ZAHRA and C. ZAHRA, *Z. Metallkde* **71** (1980) 231.

Received 2 July 1991
and accepted 7 February 1992